© 2020. Published by The Company of Biologists Ltd | Journal of Experimental Biology (2020) 223, jeb225029. doi:10.1242/jeb.225029

RESEARCH ARTICLE

Air-entrapping capacity in the hair coverage of *Malacosoma castrensis* (Lasiocampidae: Lepidoptera) caterpillar: a case study

Alexander Kovalev[1,*], Manuela Rebora[2], Gianandrea Salerno[3] and Stanislav Gorb[1]

ABSTRACT

The moth *Malacosoma castrensis* (Lasiocampidae) is commonly found along the Northern Germany coasts, the habitats of which are mainly represented by salt marshes subjected to sea level variations. Surprisingly, terrestrial caterpillars can withstand many hours of being flooded by seawater. The ability to withstand periods of submersion in a terrestrial insect raises the problem of respiration related to avoiding water percolation into the tracheal system. In the present study, we investigated under laboratory conditions the role of water-repellent cuticle structures in oxygen supply in caterpillars of *M. castrensis* submerged in water. For this purpose, air-layer stability tests using force measurements, and micromorphology of cuticle structures using SEM and fluorescence microscopy, were performed. A plastron appeared when a caterpillar is underwater. The stability, gas composition and internal pressure of the plastron were estimated. The plastron is stabilized by long and scarce hairs, which are much thicker than the corresponding hairs of aquatic insects. Thick and stiff hairs with sclerotized basal and middle regions protrude into the water through the plastron–water interface, while substantial regions of thin and flexible hairs are aligned along the plastron–water interface and their side walls can support pressure in the plastron even below atmospheric pressure. Additional anchoring points between hair's stalk and microtrichia near the hair base provide enhanced stiffness to the hair layer and prevent the hair layer from collapse and water entering between hairs. The advancing contact angle on hairs is more than 90 deg, which is close to the effective contact angle for the whole caterpillar.

KEY WORDS: Cuticle, Hydrophobicity, Plastron, Air-retaining

INTRODUCTION

On the basis of fossil records, it is generally agreed that the basal forms of modern insects were terrestrial and that aquatic insects are derived from terrestrial precursors secondarily invading aquatic environments (Wootton, 1988; Lancaster and Downes, 2013; Dijkstra et al., 2014). The transition from a terrestrial habitat to an aquatic one presents a range of specific problems for insects and requires numerous adaptations in their mechanisms of thermoregulation, osmoregulation, locomotion, feeding and respiration.

[1]Department of Functional Morphology and Biomechanics, Zoological Institute, Kiel University, Am Botanischen Garten 1-9, 24118 Kiel, Germany. [2]Dipartimento di Chimica, Biologia e Biotecnologie, University of Perugia, Via Elce di Sotto 8, 06121 Perugia, Italy. [3]Dipartimento di Scienze Agrarie, Alimentari e Ambientali, University of Perugia, Borgo XX Giugno, 06121 Perugia, Italy.

*Author for correspondence (akovalev@zoologie.uni-kiel.de)

A.K., 0000-0002-9441-5316; M.R., 0000-0002-4271-6336; G.S., 0000-0002-8357-7598; S.G., 0000-0001-9712-7953

Received 11 March 2020; Accepted 2 June 2020

Aquatic insects belong to 12 orders that invaded water multiple times. Among them, Ephemeroptera, Odonata, Plecoptera, Trichoptera and Megaloptera are almost exclusively restricted to freshwater during their larval stage. Approximately 30% of Diptera (the largest group), over 10% of the suborder Heteroptera, 3% of Coleoptera and very small proportions of Neuroptera, Orthoptera, Hymenoptera and Lepidoptera are aquatic (Dijkstra et al., 2014). This last order is primarily terrestrial, but there are a few species mainly belonging to Pyralidae and Crambidae with aquatic larvae, which show filamentous gills on their body (Stoops et al., 1998; Vallenduuk and Cuppen, 2004).

The ground lackey, *Malacosoma castrensis* (Linnaeus 1758) (Lepidoptera: Lasiocampidae), is widespread in Europe and temperate Asia (Tshistjakov, 1998; Zolotuhin, 1992) (Fig. 1A). It can be found in terrestrial regions, but tends to the tidal regions. In Europe, for example, it is missing in the southernmost regions (but occurs numerously in the northern Mediterranean) and the polar zone (Southern Scandinavia) (www.pyrgus.de/Malacosoma_castrensis_en.html) (Fig. 1B). It is a polyphagous species inhabiting warm, nutrient-poor grasslands. The adults do not feed, while caterpillars forage on a wide range of herbaceous plant species belonging to different families. The species has only one generation per year and overwinters at the egg stage. Larvae from overwintering egg masses laid around the stem of herbaceous plants hatch in early spring with the emergence and expanding of buds on host plants (Karimpour, 2018). The young larvae are gregarious and, as in other Lasiocampidae, form larval masses living in conspicuous tents of silk used as shelters and molting sites. This moth is commonly found along the Northern Germany coasts, with habitats mainly represented by salt marshes subjected to sea level variations. Here, caterpillars feed on coastal plants, such as sea plantain (*Plantago maritima*), common sea-lavender (*Limonium vulgare*) and sea wormwood (*Artemisia maritima*). In consideration of the habitat of this species, caterpillars can withstand many hours of being flooded by the seawater.

The ability to withstand periods of submersion in a terrestrial insect raises the problem of respiration related to avoiding water invasion into the tracheal system. Some aquatic insects, such as marine Heteroptera, living at the boundary between air and water, and resisting immersion for short, but regular periods of time, developed a cuticle that is rich of dense setae inserted in sockets and short subcellular filiform protuberances (microtrichia) able to retain a thin layer of air on the cuticle during submersion (Perez-Goodwyn, 2009; Balmert et al., 2011).

In the present study, we investigated under laboratory conditions water-repellent cuticle structures, which allow caterpillars of the terrestrial moth *M. castrensis* to retain atmospheric oxygen when submerged in water. For this purpose, air-layer stability tests using force measurements were performed. To analyze the structure of caterpillar hairs in relation to their possible involvement in air retaining, we performed an ultrastructural analysis with scanning electron microscopy (SEM). The presence and distribution of the elastic protein resilin as

Journal of Experimental Biology (2020) 223, jeb225029. doi:10.1242/jeb.225029

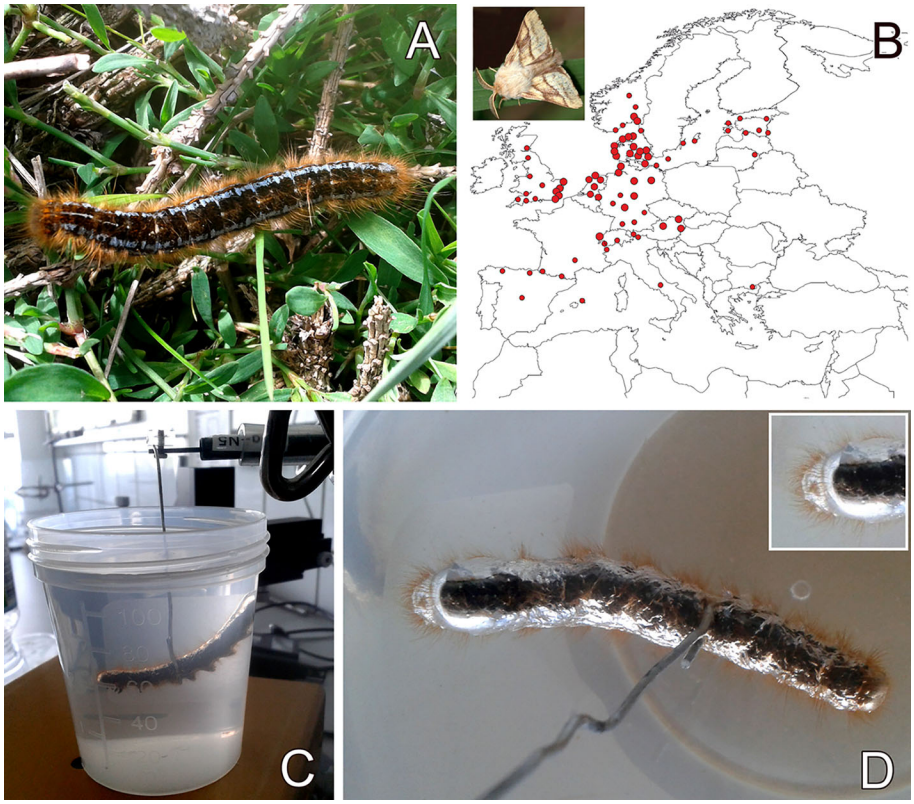

Fig. 1. *Malacosoma castrensis*, its areal distribution and the buoyancy experimental setup. (A) *M. castrensis* caterpillar in its natural habitat. (B) Areal distribution (data from www.beachexplorer.org/arten/malacosoma-castrensis-larva/verbreitung). Inset shows an adult moth. (C) Experimental setup for measuring buoyancy force. (D) Buoyancy measurement, view from above. Inset shows an enlarged image of the caterpillars' head 1 min after the beginning of the experiment.

well as the distribution of sclerotization degree in the cuticle of these structures were revealed by fluorescence microscopy.

MATERIALS AND METHODS

Insects

Two caterpillars of the ground lackey, *M. castrensis*, belonging to the penultimate and ultimate stages were collected in June 2017 at the North Sea shore in the salt marsh vegetation near Westerhever (Schleswig-Holstein, Germany) on sea grasses (*Seriphidium maritimum*, *Limonium vulgare*) growing in the area around the lighthouse. This area is flooded twice a day for approximately 1 to 6 h. Length and mass of the caterpillars were 44.6 and 46.7 mm, and 0.797 and 0.839 g, respectively.

Buoyancy force measurements

The experiments set up for a caterpillar buoyancy characterization consisted of a FORT-10 force transducer (10 g capacity; World Precision Instruments Inc., Sarasota, FL, USA) connected to an MP 100 amplification and digitalization system (Biopac Systems Ltd, Goleta, CA, USA) (Gorb et al., 2010; Zheden et al., 2015). Data were recorded using AcqKnowledge 3.7.0 software (Biopac Systems Ltd, Goleta, CA, USA). A caterpillar was attached to the force transducer using a metal wire (Fig. 1C,D). It was submerged then for some time (from 1 min to 13 h) underwater. The animals were alive after all the submerging experiments were carried out. The buoyant force was measured during this procedure. Six separate experiments on two individual animals were performed. The variations of the measured force arise because of the changes in the volume of the air layer surrounding the caterpillar.

Scanning electron microscopy

Air-dried samples of the hairs of *M. castrensis* caterpillars were mounted on aluminium holders, sputter-coated with gold-palladium (10 nm) and studied using a Hitachi S-4800 scanning electron microscope (Hitachi High-Technologies Corp., Tokyo, Japan) at an acceleration voltage of 3 kV. The mixture of signals from upper and lower detectors was used to produce images. For further details of the sample preparation and the mounting for SEM imaging, see Gorb and Gorb (2009).

Fluorescence microscopy

Fluorescence microscopy was used to reveal some differences in the molecular composition along the caterpillar setae, which are basically cuticular outgrowths. Different constituents of insect cuticle are well known to have a spectrally specific autofluorescence. In contrast to tanned sclerotized cuticle, which usually demonstrates red fluorescence by 488 nm excitation, the rubber-like cuticular protein resilin possesses a narrow band autofluorescence at approximately 420 nm by 405 nm excitation (Andersen and Weis-Fogh, 1964). To prevent photobleaching, setae were mounted in a water-soluble medium (Moviol) on a glass slide and covered with a coverslip (Haas et al., 2000). Autofluorescence images were obtained using a Zeiss Axioplan conventional fluorescence microscope (Oberkochen, Germany) equipped with an AxioCam MRc camera and light source with an HBO 100 W lamp. The autofluorescence was registered in three wavelength bands: UV band (excitation 320–380 nm, emission 420–470 nm), green (excitation 450–490 nm, emission >520 nm) and red (excitation 535–560 nm, emission >590 nm). Fluorescence images, taken in three different spectral ranges, were superimposed and assigned to the three color channels, in order to reveal local differences in the cuticle composition.

RESULTS

Buoyancy force measurements

An unusual behavior of *M. castrensis* caterpillars was observed in the field. Unlike caterpillars of other species from this genus

Journal of Experimental Biology (2020) 223, jeb225029. doi:10.1242/jeb.225029

that immediately leave their plant substrate when submerged, *M. castrensis* caterpillars stop moving, clinging to the plant. During the high tide at North Sea coasts, they can survive being submerged under salt water for 1–8 h twice a day without the presence of a specialized gill, called a plastron. This observation led us to assume that the caterpillars have specific adaptations to survive tide periods and cling to the plant, in order to prevent being taken away by the sea.

In the buoyancy experiment, the force during submergance of the caterpillar in seawater was recorded. This force (F_m) is the difference between gravitational (F_g) and push-out (F_p) forces: $F_m=F_g–F_p$ (Fig. 2). Because the gravitational force is constant (Fig. 2A and the left diagram in Fig. 2B), the measured force curve characterizes the change in the push-out force, which reaches its maximum at some particular dip depth (Fig. 2A and the middle diagram in Fig. 2B). When the caterpillar is completely underwater, the push-out force remains constant, and tiny force variations are correlated with the change in the volume of the caterpillar and the air bubble around it, which can be recognized because of the total internal reflection from the water–air interface when the observation angle exceeds 49 deg (mirror-like reflection in Fig. 1D).

The volume of a caterpillar and the air around it can be estimated from Archimedes' principle. After several hours underwater, this volume was 960.6±3.0 µl (mean±s.e.m.) (Fig. 2A). It was calculated from the caterpillars' length (44.71±0.05 mm) under the assumption that the caterpillar has a cylindrical shape and a diameter-to-length ratio (or projection area to length squared ratio) equal to 0.117 (Fig. 1A). Effective density can be calculated as mass-to-volume ratio. For the two investigated caterpillars, their effective densities were 818 and 856 kg m^{-3}. The maximum caterpillar volume immediately after submerging it in water was 1335 µl; assuming homogeneous distribution of the air around the caterpillar body, this corresponds to a 468 µm thick air layer. From two long-lasting experiments, disappeared air volumes were 237 µl (within 46 min experiment) and 276 µl (within 13 h experiment), which correspond to 298 µm and 359 µm of the air layer thickness, respectively. Such air loss is known to happen, since air layer under water is at higher than atmospheric pressure, and therefore it is in a metastable state. The air permanently diffuses into/out of water through air–water interfaces. The diffusional dissolution rate of the plastron gas (ratio of the gas volume loss per surface area per time) was very different in different experiments (0.5 to 7.8 mmol m^{-2} h^{-1}) as estimated from the linear regression of the time-volume decay (Fig. 2C).

Another mechanism of air loss from the plastron is a spontaneous, quick (within 1 s) bubble separation (Fig. 2A). The mean bubble diameter was 5.34±0.30 mm, which is comparable with the caterpillar diameter and corresponds to the ∼100 µm decrease of the effective air layer thickness. The air bubbles separate from the plastron within 10 min of the caterpillar submerging, with a geometric mean time of 110 s. In one of the experiments, we observed that a bubble 2 mm in diameter joined the plastron. Bubbles like this often appeared on the vessel walls and bottom, when the ambient temperature increased. However, the gas volume change in the plastron, because of the temperature variation in the laboratory during experiments (less than 4°C), was negligible.

Some interesting events of sudden volume increase and further exponential decay to the previous volume value were observed for the first hour of caterpillar submergence (Fig. 2C). The mean volume variation was 88±32 µl, and the geometric mean recovery time was 14.0 s (4.2 to 319.0 s). After the first hour of caterpillar submergence, similar but slower volume variations were observed with almost linear volume increase and following exponential volume decay (Fig. 2A). For two such events, the mean volume

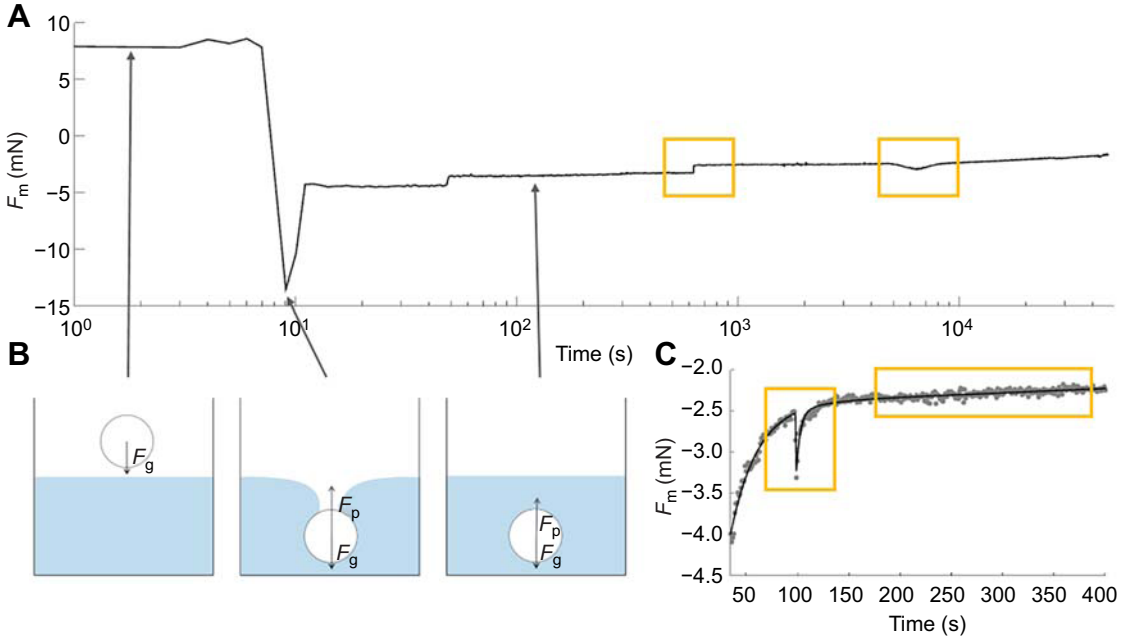

Fig. 2. A typical buoyancy experiment. (A) Force dynamics during the experiment, presented in a logarithmic time scale. F_m, net measured force. The force–time curve (A) is shown with the three important phases, indicated by arrows, of the dip process (B): (1) caterpillar has no contact with water, (2) highly curved meniscus is formed around the caterpillar body, and (3) caterpillar is completely under the water. The circle corresponds to the cross-section of the caterpillar body. F_g and F_p are the gravitational and push-out forces, respectively. A sudden force jump and a slow reversible force change are marked with (correspondingly left and right) boxes on the force–time curve. A section of the force–time curve shown in C represents a slow exponential force relaxation (volume decay), when caterpillar was completely under the water (the right subplot in B). Measurements are shown as gray dots, fit is shown as a solid line. Left and right boxes mark a fast relaxation process with small amplitude and a linear force increase (volume decay), respectively.

Journal of Experimental Biology (2020) 223, jeb225029. doi:10.1242/jeb.225029

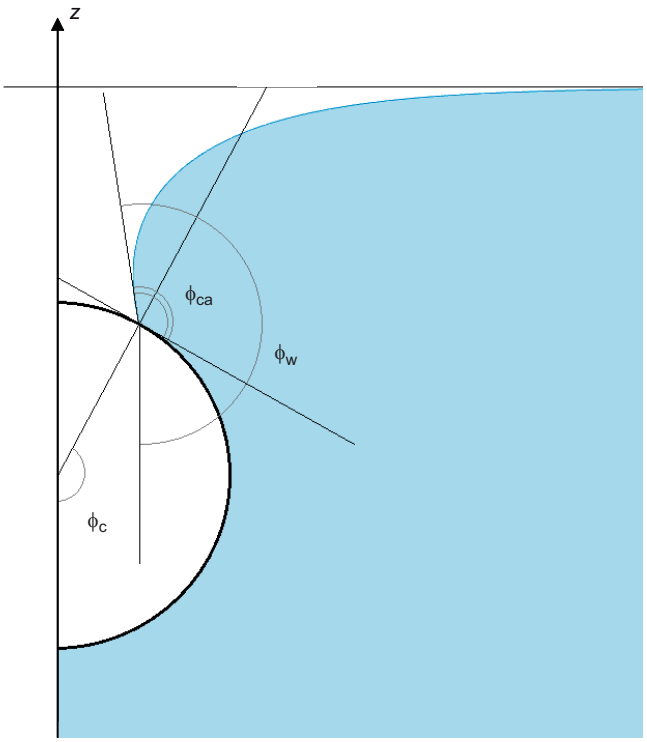

Fig. 3. Cylindrical body (just one half is shown) submerged in water (shown in blue). The undisturbed water level is at z=0, ϕ_{ca} is the water contact angle, ϕ_c is the angle between the z-axis and a line going through the center of cylinder and the point of the water meniscus contact on the cylinder, and ϕ_w is the angle between the water meniscus surface and a vertical.

increase speed was 71 µl h^{-1}, the mean volume variation was 39 µl and the geometric mean recovery time was 20 min.

During dipping a cylinder with its side in water, the menisci may produce forces comparable with the gravitational forces. General push-out (buoyant) force, which acts on a cylindrical body, is determined by the following equation:

$$F_p = F_t + F_b = 2L\gamma\sin\varphi_w + \rho g R L(R\varphi_c + (2h - R\cos\varphi_c)\sin\varphi_c), \quad (1)$$

where F_t is the surface tension force, F_b is the buoyancy force (the difference between forces acting on the lower and upper surfaces of the cylindrical body), L is the cylinder length, γ is the surface tension (γ=73.3 mN m^{-1}, calculated according to Naya et al., 2014), ϕ_c and ϕ_w are the water contact angle and the angle between the water meniscus at depth h and a vertical line, respectively, ρ is the water density (for seawater, ρ=1022 kg m^{-3}, calculated according to an equation presented in Fofonoff and Millard, 1984), g is the gravitational acceleration (g=9.813 m^2 s^{-1}), and R is the radius of the cylinder (Fig. 3). After a straightforward conversion of equations presented in Zheng et al. (2009), the dependency of ϕ_w on h can be expressed as:

$$\varphi_w = tg^{-1}\left(\frac{h\sqrt{4\gamma/(\rho g) - h^2}}{h^2 - 2\gamma/(\rho g)}\right) + \pi/2 + \pi\theta\left(h - \sqrt{2\gamma/(\rho g)}\right), \quad (2)$$

where θ is the step function [$\theta(x)$=0, $x\leq$0; $\theta(x)$=1, x>0].

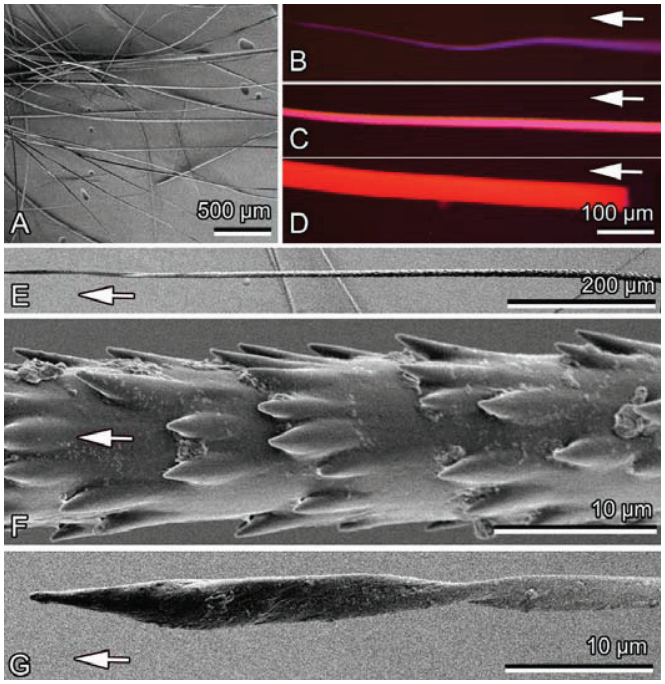

Fig. 4. Morphology of setae from the *M. castrensis* caterpillar body. (A) Air-dried setae. (B,G) Setal tips. (C,E) Middle region of the seta. (D,F) Basal region of the seta. A,E–G are scanning electron microscopy images; B–D are composed autofluorescence images. Arrows indicate distal direction.

The push-out force reaches its maximum at some particular dip depth (Fig. 2A,B). From the known caterpillar dimensions and the maximum value of the push-out force, the effective water contact angle on the caterpillar can be estimated using Eqns 1 and 2. The effective contact angle for a caterpillar was equal to 98.3±11.7 deg.

Setae morphology

The hairs (setae) at their base are cylindrical and supplemented by microtrichia pointing to the tip of the hair (Fig. 4A,E,F). The very top of the hairs is flattened and slightly coiled, and has no microtrichia (Fig. 4E,G). The longest hair length was around 3 mm (Fig. 1A). The diameter in the middle area of hairs strongly varies, from 7 to 25 µm; therefore, their shape varies from filiform to stiff and straight, correspondingly.

The base of hairs demonstrates enhanced autofluorescence in the red spectral range (emission >590 nm), while the tip of hairs demonstrates enhanced autofluorescence in the blue spectral range (emission 420–470 nm) (Fig. 4B,D). The receding and advancing contact angles are slightly below and slightly above 90 deg, respectively.

DISCUSSION

Air-retaining surfaces are known from different arthropods, aquatic birds, aquatic plants and some other organisms (Barthlott et al., 2010; Ditsche-Kuru et al., 2011; Marx and Messner, 2012; Ditsche et al., 2015; see review in Barthlott et al., 2016). Among insects, according to the different grade of adaptation to aquatic habitats (species living close to water in air, at a middle point between water and air, or underwater), different levels of air-retention capability can be envisaged (Perez-Goodwyn, 2009; Balmert et al., 2011). However, primarily terrestrial species usually do not possess such highly specialized surfaces. The present study reports on the air-entrapping capacity in the hair coverage of the primarily terrestrial caterpillar *M. castrensis*. This adaptation provides some selective advantage to this species in occupying intertidal habitats of the North Sea.

Journal of Experimental Biology (2020) 223, jeb225029. doi:10.1242/jeb.225029

In aquatic insects, the plastron is supported by a dense layer of specialized thin hairs, while the hairs in caterpillars are much thicker, have a higher aspect ratio and are less dense. Caterpillar hairs were previously demonstrated to provide several different functions. They simply build a physical barrier as a defense mechanism against natural enemies, as was shown for caterpillars of *Lemyra imparilis* (Lepidoptera: Erebidae) and *Lymantria dispar japonica* (Lepidoptera: Erebidae), for which hair length is of high importance in defense against predation by carabid beetles (Sugiura and Yamazaki, 2014). Additionally, both hair length and thickness are important factors in defense of *L. d. japonica* against oviposition by the endoparasitoid *Meteorus pulchricornis* (Hymenoptera: Braconidae) (Kageyama and Sugiura, 2016). The hairs may be involved in the perception of the motion of the surrounding medium, as previously reported for the cabbage moth caterpillar *Mamestra brassicae* (Lepidoptera: Noctuidae), which can sense sound stimuli at low frequency and respond with a defensive reaction (Markl and Tautz, 1975). Finally, the hairs might prevent drowning of caterpillars, as was shown for *L. imparilis* (Meyer-Rochow, 2016).

Most terrestrial insects placed underwater start to actively move, trying to reach the air–water interface. In caterpillars of tidal *M. castrensis*, other specific behavior is observed: once underwater, they cling to the substrate with their attachment devices and stay motionless (S.G., personal observations). For the caterpillars, it is obviously advantageous to stay through the high tide on the host plants. Because the body density of *M. castrensis* is approximately 840 kg m^{-3}, if they are released from the plant, they would stay on the water surface. Floating on the water surface is a high risk for the caterpillars, because they may be driven by water current into the open sea or collected by water birds.

Interestingly, the caterpillar radius is almost equal to the capillary length (2.7 mm in our case). This may be related to the smallest shear forces on a cylinder with a radius equal to capillary length produced by water running on the hydrophobic plant surface (e.g. *A. maritima*), when the water level increases during high tide. To prevent caterpillar suffocation underwater, it should possess a kind of a plastron for effective CO_2 exchange. Assuming that the volume of the tracheal system in *M. castrensis* caterpillars is similar to that previously studied in *Manduca sexta* (Lepidoptera: Sphingidae), which is ∼7.5% of the caterpillar volume (Helm and Davidowitz, 2013), we can approximate the tracheal volume for our caterpillars as 72 µl. A plastron is obviously present in *M. castrensis* caterpillars underwater. The volume of the plastron decreases with time. The maximal measured air volume disappeared from the plastron was 375 µl, which is approximately five times the tracheal volume.

There are two main mechanisms of the plastron volume decay: bubble separation and air diffusion from the plastron, where the air pressure is higher than the atmospheric pressure, through the water. Bubbles separated from the plastron reduce its volume and the time the caterpillar may stay underwater.

The effective diffusion constant for the air leakage from the plastron could be estimated from Henry's and Fick's first laws (Henry, 1803; Fick, 1855). Assuming that a stable concentration gradient of dissolved gases is formed in a thin water layer close to the plastron, the gas transfer rate, v, through the gas–water interface could be found from the following equation:

$$v = ADH_{cp}\frac{p_{pl} - p_{atm}}{\delta}, \quad (3)$$

where A is the surface area of the gas–water interface, D is the diffusion constant of gas in water, H_{cp} is the gas solubility constant, δ is the diffusion layer thickness, and p_{atm} and p_{pl} are the partial pressures of a gas in the atmosphere and plastron, respectively. The gas transfer rates at some interesting parameter combinations calculated using Eqn 3 are presented in Table 1. The diffusion layer thickness was taken equal to 0.5 mm, according to Seymour et al. (2015), and all the parameters were normalized for experimental conditions at 20°C.

Table 1. Particular gas transfer rates through the gas–water interface

Gas	H_{cp} [µmol (Pa·m^3)$^{-1}$]	D (m^2 s^{-1})	p_{pl}–p_{atm} (kPa)	v (µmol h^{-1})
CO_2	330	1.92×10^{-9}	1	3.36
O_2	12	2.10×10^{-9}	−19.3	−2.58
N_2	6.4	1.88×10^{-9}	18.3	1.17

H_{cp}, gas solubility constant; D, diffusion constant of gas in water; p_{atm} and p_{pl}, the partial pressures of a gas in the atmosphere and plastron, respectively; v, gas transfer rate. H_{cp} and D values were taken from Sander et al. (2015) and Ferrel et al. (1967), respectively (at 737 mm^2 interface area).

During respiration, oxygen in the plastron is converted at a constant rate into CO_2. CO_2 has a transfer rate comparable with that for oxygen at ∼1 kPa partial pressure difference (Table 1). The CO_2 transfer rate at 1 kPa partial pressure is also comparable with the minimal CO_2 emission rate of ∼3 µmol h^{-1} (in *M. sexta* with 0.2–2 g body mass; Seymour et al., 2015). At such a metabolism rate, the oxygen from the plastron and tracheal system together is enough just for 1 h respiration without gas exchange between the plastron and the surrounding water. This means that permanent oxygen diffusion into the plastron is taking place (Fig. 5). Stationary O_2 partial pressure should be above 2 kPa (see Seymour et al., 2015) to maintain the oxidative process in the mitochondria.

Assuming stationary gas concentrations and diffusion, all of the nitrogen should diffuse out of the plastron (and the plastron should disappear) in approximately 7.6 h. Because the caterpillars in our experiment possessed plastron even after 13 h underwater, a cuticular hydrophilic structure should exist, which can suspend the gas–water interface at the pressure in the plastron, which is less than 93.7 kPa (for 101.3 kPa atmospheric pressure). Therefore, in the case of *M. castrensis* caterpillars, one may consider the presence of an incompressible physical gas gill (Seymour and Matthews, 2013). Summing up, the oxygen permanently diffuses into the plastron and is converting during respiration into CO_2, which diffuses out of the plastron. Nitrogen basically diffuses out of the plastron until the pressure drops below atmospheric pressure (Fig. 5).

The gas transfer rates in tidal seawater should be much higher, as the diffusion layer thickness depends on the water flow velocity, and already for ∼6 mm s^{-1} velocity it is five times less than for standing water (Seymour et al., 2015).

A single event of the sudden significant gas volume increase (∼90 µl, Fig. 2C) cannot be related to muscle contraction or to the change in internal hydrostatic pressure, but may be associated with bacterial activity in the caterpillar gut. However, small reversible

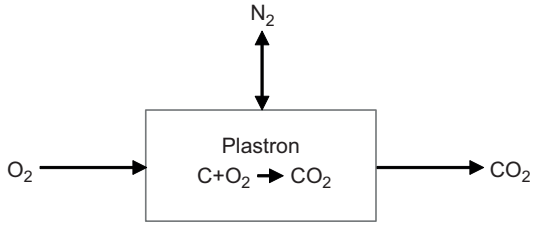

Fig. 5. Gas balance in the plastron depends on respiration and gas exchange between the plastron and the surrounding water.

changes of the caterpillar volume at different time intervals (Fig. 2A) might be related to the tonal muscle contraction.

At the initial stage of the caterpillar submerging in water, the hairs on the cuticle of *M. castrensis* are responsible for the enlarged volume of the plastron and prevent the contact of water with the animal body (Fig. 1D). The hairs have advancing contact angles of more than 90 deg, which explains the high value of the effective macroscopic contact angle of caterpillars during dipping, 98 deg. The plastron volume is also stabilized by hairs. Thick and stiff hairs protrude into the water through the plastron–water interface and stabilize it at shear stress in turbulent water flow. The middle and basal regions of the hairs are rigid, because they are thickened and sclerotized (Fig. 4D, red fluorescence). Thin hairs are more flexible. Especially flexible is their distal part, which is flattened and demonstrates bluish autofluorescence (Fig. 4B), which is characteristic for the cuticle enriched with resilin (rubber-like soft protein) (Haas et al., 2000). Because thin hair tips are extremely flexible and their advancing contact angle is more than 90 deg, they cannot penetrate the plastron–water interface. Substantial regions of thin hairs are aligned along the plastron–water interface and can support menisci with even negative curvature (when the pressure in the plastron is below atmospheric pressure), resembling hair-like structures (trichomes) on the leaves of the underwater fern *Salvinia oblongifolia* (Barthlott et al., 2010; Ditsche et al., 2015). Additionally, interlocking of the hair's stalk and tip with microtrichia located near the hair base (Fig. 4E,F) provides enhanced stiffness to the hair layer and prevents the hair layer from collapse and water entering between hairs. The twist of the flattened hair tip ensures its proper orientation for interlocking with microtrichia and is responsible for reduction of the contact area of the tip with water. Anisotropic orientation of microtrichia presumably hinders the water meniscus motion into the direction of the hair base, because the water–air interface is disturbed by the microtrichia tips. Therefore, the motion of the water–air interface against the microtrichia requires more energy than its motion along the microtrichia or equivalent conical structure, or even along a smooth hair. Microtrichia on a hair along the water–air interface increase the interface deformation.

Conclusions

Caterpillars of *M. castrensis* may be regarded as terrestrial animals; however, possession of specific structures and behavioral adaptations allow them to survive on plants in a tidal zone. It is still an open question as to which other adaptations for this specific habitat they have. Here, we investigated some properties of the plastron, which allows caterpillars of *M. castrensis* to survive many hours underwater. The plastron of *M. castrensis* is different from the typical plastron of aquatic insects. In the majority of aquatic insects, the plastron is supported by a dense layer of specialized thin hairs, whereas the hairs in *M. castrensis* caterpillars are much thicker, have a higher aspect ratio and are much less dense. The caterpillar plastron is stabilized by hair sidewalls similar to those of aquatic insects, described in Flynn and Bush (2008). The pressure in the caterpillar plastron can be less than 92% of atmospheric pressure. The plastron may withstand both hydrostatic and hydrodynamic pressure in tidal water currents.

However, future studies on different larval instars of *M. castrensis*, as well as other closely related species of *Malacosoma* moths that do not live in such a specific habitat as *M. castrensis*, should be performed, in order to understand the selective advantages of the morphological and behavioral features of these caterpillars in further detail. Also, exploring caterpillars of other lepidopteran species, living in habitats similar to those of *M. castrensis*, would be important to reveal convergent evolution of the hairy covering of the larval body.

Similar to other superhydrophobic plastron-bearing biological surfaces (Busch et al., 2019), our results on the caterpillar plastron may find its applications in marine technology owing to its ability to maintain air bubbles for drag reduction and anti-fouling. Additionally, as suggested by Shirtcliffe et al. (2006), submerged cavities consisting of specially designed hydrophobic material might provide oxygen necessary to run fuel cells to supply power to small underwater vehicles through a mechanism analogous to plastron respiration.

Competing interests

The authors declare no competing or financial interests.

Author contributions

Conceptualization: A.K., M.R., G.S., S.G.; Methodology: A.K., M.R., G.S., S.G.; Software: A.K.; Validation: M.R., G.S., S.G.; Formal analysis: A.K., S.G.; Investigation: A.K., M.R., G.S., S.G.; Resources: S.G.; Data curation: S.G.; Writing - original draft: A.K., M.R.; Writing - review & editing: A.K., M.R., G.S., S.G.; Visualization: A.K., M.R., G.S., S.G.; Supervision: G.S., S.G.; Project administration: S.G.; Funding acquisition: M.R., G.S., S.G.

Funding

This study was funded by Deutscher Akademischer Austauschdienst, Research Stays for University Academics and Scientists, 2019 (57440915).

References

Andersen, S. O. and Weis-Fogh, T. (1964). Resilin, a rubber-like protein in arthropod cuticle. *Adv. InsectPhysiol.* **2**, 1-65. doi:10.1016/S0065-2806(08)60071-5

Balmert, A., Bohn, H. F., Ditsche-Kuru, P. and Barthlott, W. (2011). Dry under water: comparative morphology and functional aspects of air-retaining insect surfaces. *J. Morphol.* **272**, 442-451. doi:10.1002/jmor.10921

Barthlott, W., Schimmel, T., Wiersch, S., Koch, K., Brede, M., Barczewski, M., Walheim, S., Weis, A., Kaltenmaier, A., Leder, A. et al. (2010). The *Salvinia* paradox: superhydrophobic surfaces with hydrophilic pins for air retention under water. *Adv. Mater* **22**, 2325-2328. doi: 10.1002/adma.200904411

Barthlott, W., Mail, M. Neinhuis, C. (2016). Superhydrophobic hierarchically structured surfaces in biology: evolution, structural principles and biomimetic applications. *Phil. Trans. R. Soc. A* **374**, 1-41. doi: 10.1098/rsta.2016.0191

Busch, J., Barthlott, W., Brede, M., Terlau, W. and Mail, M. (2019). Bionics and green technology in maritime shipping: an assessment of the effect of *Salvinia* air-layer hull coatings for drag and fuel reduction. *Phil. Trans. R. Soc. A* **377**, 20180263. doi:10.1098/rsta.2018.0263

Dijkstra, K. D., Monaghan, M. T. and Pauls, S. U. (2014). Freshwater biodiversity and aquatic insect diversification. *Ann. Rev. Entomol.* **59**, 143-163. doi:10.1146/annurev-ento-011613-161958

Ditsche-Kuru, P., Schneider, E. S., Melskotte, J.-E., Brede, M., Leder, A. and Barthlott, W. (2011). Superhydrophobic surfaces of the water bug *Notonecta glauca*: a model for friction reduction and air retention. *Beilstein J. Nanotechn* **2**, 137-144. doi: 10.3762/bjnano.2.17

Ditsche, P., Gorb, E. V., Mayser, M., Gorb, S. N., Schimmel, T. and Barthlott, W. (2015). Elasticity of the hair cover in air-retaining *Salvinia* surfaces. *Applied Physics A* **121**, 505-511. doi:10.1007/s00339-015-9439-y

Ferrell, R. T. and Himmelblau, D. M. (1967). Diffusion coefficients of nitrogen and oxygen in water. *J. Chem. Eng. Data* **12**, 111-115. doi:10.1021/je60032a036

Fick, A. (1855). Ueber diffusion. *Annal. Phys.* **94**, 59-86. doi:10.1002/andp.18551700105

Flynn, M. R. and Bush, J. W. M. (2008). Underwater breathing: the mechanics of plastron respiration. *J. Fluid Mech.* **608**, 275-29681. doi:10.1017/S0022112008002048

Fofonoff, N. P. and Millard, R. C., Jr. (1984). Algorithms for computation of fundamental properties of seawater. Paris, UNESCOTech. *Pap. Mar. Sci.* **44**, 17.

Gorb, E. V. and Gorb, S. N. (2009). Functional surfaces in the pitcher of the carnivorous plant *Nepenthes alata*: a cryo-SEM approach. In *Functional Surfaces in Biology - Adhesion Related Phenomena*, Vol. 2 (ed. S. N. Gorb), pp. 205-238. Dordrecht, Heidelberg, London, New York: Springer.

Gorb, E. V., Hosoda, N., Miksch, C. and Gorb, S. N. (2010). Slippery pores: anti-adhesive effect of nanoporous substrates on the beetle attachment system. *J. Royal Soc. Interface* **7**, 1571-1579. doi:10.1098/rsif.2010.0081

Haas, F., Gorb, S. N. and Blickhan, R. (2000). The function of resilin in beetle wings. *Proc. R. Soc. London B* **267**, 1375-1381. doi:10.1098/rspb.2000.1153

Helm, B. R. and Davidowitz, G. (2013). Mass and volume growth of an insect tracheal system within a single instar. *J. Exp. Biol.* **216**, 4703-4711. doi:10.1242/jeb.080648

Henry, W. (1803). Experiments on the quantity of gases absorbed by water, at different temperatures, and under different pressures. *Phil. Trans. R. Soc. Lond* **93**, 29-274. doi:10.1098/RSTL.1803.0004

Kageyama, A. and Sugiura, S. (2016). Caterpillar hairs as an anti-parasitoid defence. *Sci. Nat.* **103**, 86. doi:10.1007/s00114-016-1411-y

Karimpour, Y. (2018). Notes on life history, host plants and parasitoids of *Malacosoma castrensis* L. (Lepidoptera: Lasiocampidae) in Urmia region. Iran. *Biharean Biologist* **12**, e171209.

Lancaster, J. and Downes, B. J. (2013). *Aquatic Entomology*, pp. 296. Oxford: Oxford University Press.

Markl, H. and Tautz, J. (1975). The sensitivity of hair receptors in caterpillars of *Barathra brassicae* L (Lepidoptera, Noctuidae) to particle movement in a sound field. *J Comp. Physiol.* **99**, 79-87. doi:10.1007/BF01464713

Marx, M. T. and Messner, B. (2012). A general definition of the term “plastron“ in terrestrial and aquatic arthropods. *Org. Divers Evol.* **12**, 403-408. doi: 10.1007/s13127-012-0088-0

Meyer-Rochow, V. B. (2016). Depilation increases while hairiness decreases the risk of drowning: a hitherto unappreciated survival role of setae in woolly bear caterpillars of the moth *Lemyra imparilis* (Lepidoptera: Noctuoidea: Erebidae). *Eur. J. Entomol.* **113**, 130-134. doi: 10.14411/eje.2016.016

Naya, K. G., Panchanathan, D. and McKinley, G. H. (2014). Surface tension of seawater. *J. Phys. Chem. Data* **43**, 043103. doi: 10.1063/1.4899037

Perez-Goodwyn, P. (2009). Anti-wetting Surfaces in Heteroptera (Insecta): Hairy solutions to any problem. In *Functional Surfaces in Biology* (ed. S. N. Gorb), pp. 55-76. Dordrecht: Springer.

Sander, R. (2015). Compilation of Henry’s law constants (version 4.0) for water as solvent. *Atmos. Chem. Phys*. **15**, 4399-4981. doi:10.5194/acp-15-4399-2015

Seymour, R. S. and Matthews, P. G. D. (2013). Physical gills in diving insects and spiders: theory and experiment. *J. Exp. Biol.* **216**, 164-170. doi:10.1242/jeb.070276

Seymour, R. S., Jones, K. K. and Hetz, S. K. (2015). Respiratory function of the plastron in the aquatic bug *Aphelocheirus aestivalis* (Hemiptera, Aphelocheiridae). *J. Exp. Biol.* **218**, 2840-2846. doi:10.1242/jeb.125328

Shirtcliffe, N. J., McHale, G., Newton, M. I., Perry, C. C. and Pyatt, F. B. (2006). Plastron properties of a superhydrophobic surface. *Appl. Phys. Lett*. **89**, 104106. doi:10.1063/1.2347266

Stoops, C. A., Adler, P. H. and McCreadie, J. W. (1998). Ecology of aquatic Lepidoptera (Crambidae: Nymphulinae) in South Carolina, USA. *Hydrobiologia* **379**, 33-40. doi:10.1023/A:1003269025247

Sugiura, S. and Yamazaki, K. (2014). Caterpillar hair as a physical barrier against invertebrate predators. *Behav. Ecol.* **25**, 975-983. doi:10.1093/beheco/aru080

Tshistjakov, Y. A. (1998). New data on the lappet-moths (Lepidoptera, Lasiocampidae) of the Russian Far East. *Far Eastern Entomologist* **66**, 1-8.

Vallenduuk, H. J. and Cuppen, H. M. J. (2004). The aquatic living caterpillars (Lepidoptera: Pyraloidea: Crambidae) of Central Europe. A key to the larvae and autecology. *Lauterbornia* **49**, 1-17.

Wootton, R. J. (1988). The historical ecology of aquatic insects: an overview. *Palaeogeogr. Palaeoclimatol. Palaeoecol.* **62**, 477-492. doi:10.1016/0031-0182(88)90068-5

Zheden, V., Kovalev, A., Gorb, S. N. and Klepal, W. (2015). Characterization of cement float buoyancy in the stalked barnacle *Dosima fascicularis* (Crustacea, Cirripedia). *Interface Focus* **5**, 20140060. doi: 10.1098/rsfs.2014.0060

Zheng, Q., Yu, Y. and Feng, X. (2009). The role of adaptive-deformation of water strider leg in its walking on water. *J. Adh. Sci. Tech.* **23**, 493-501. doi:10.1163/156856108X379155

Zolotuhin, V. V. (1992). An annotated checklist of the Lasiocampidae of European Russia (Lepidoptera). *Atalanta* **23**, 519-529.